

# Feature Identification of Solar Spectra

Samuel English<sup>1,\*</sup>

<sup>1</sup>*Department of Physics, University of California, Santa Cruz, CA 95064, USA*

(Dated: May 17, 2021)

Stellar photospheric composition remains a subject of major interest in the astrophysical community; for example, detection and quantification of new minor chemical species fills a good portion of current research [6]. Using Santa Barbara Instrument Group’s (SBIG) Self Guided Spectrograph (SGS) and spectra analysis software [4], we attempt to recover previously established results for the photosphere of our Sun. With our  $\frac{1}{d} = 600$  lines per mm, high resolution grating, Littrow geometry configuration [5], and a mercury-argon lamp for calibration we conclusively rediscover the presence of a calcium-II doublet, a sodium doublet (fine structure splitting of excited states), Balmer series emission lines, iron and magnesium absorption, as well as markers of molecular oxygen (Fig. 2). This confirms previous results [2]: the Sun’s photosphere is composed (in part) of singly-ionized calcium, hydrogen, magnesium, iron, sodium, and oxygen (Fig. 1), with a disregard for relative abundance in the scope of this paper. Relative errors are tabulated between measured and literature wavelengths for each solar feature (with associated focal length  $f$  & central angle  $\theta$ ): values do not breach 0.025%.

## I. INTRODUCTION

In this paper we will discuss: the underlying theory behind calibration of spectra (IA), how micrometer settings affect wavelength calculation (IB), the use of Fraunhofer lines in identifying solar spectral features (IC), the many sources of error potentially plaguing our results (ID); later, in our procedure, we list in detail the methods implemented to obtain the wavelengths associated with any absorption line visible (II); subsequently, in results, we describe our tabulated values and appendix plots (III A), discuss the implications of our findings on solar photospheric composition (III B); lastly, we conclude and look to future works for improvement of our results (IV).

Our goal with this experiment is to measure the spectrum of electromagnetic (EM) radiation from the sun at a high resolution diffraction grating and subsequently identify the elements which compose the sun’s photosphere.

To achieve this, we do the following: after illuminating the entrance slit of a grating spectrometer (18  $\mu\text{m}$  effective width, 600 grating lines per mm, 2.2  $\text{\AA}$  resolution, roughly 1.07  $\text{\AA}$  per pixel, and an 800  $\text{\AA}$  range dispersion [4]) with sunlight transmitted via. glass diffuser, each partial solar spectrum is recorded with our CCD detector and stored online.

For each partial spectrum, we adjust the grating tilt by means of a calibrated micrometer (setting is approximately proportional to the wavelength of EM radiation falling onto the center of the CCD detector with correspondence 1 mm to 1000  $\text{\AA}$ ). For example, to center a spectrum at 5500  $\text{\AA}$  with the high resolution grating mentioned, we set the micrometer to 5.50 mm.

Each spectrum taken has been ensured that the peak charge in any given pixel does not exceed around 30,000

units (such that the detector is kept linear as long as the charge is kept to about half the maximum digitization).

Furthermore, we took care to minimize photon bleeding due to background sources (as well as thermal sources), by covering the spectrometer with a black cloth when calibrating each configuration with a mercury lamp. In total, we dealt with seven, separate solar spectra at the following center wavelengths: 4000, 4400, 4800, 5200, 6000, 6400, 6800, and 7200  $\text{\AA}$ .

### A. Calibration Calculations

We will make use of the fundamental grating equation:

$$\sin(\theta_i) - \sin(\theta_d(\lambda)) = \frac{m\lambda}{d \cos \psi} \quad (1)$$

where  $\theta_i$  and  $\theta_d$  are *projections* of the incident and diffracted rays onto the plane of diffraction, and  $\psi$  is the out-of-plane projection angle. Due to the incident light rays all being parallel,  $\theta_i$  is actually *fixed* for each grating tilt angle with the micrometer screw ( $\psi \equiv 6.35^\circ$ ).

Our experiment’s spectrometer employs a Littrow geometry configuration in which the central diffracted ray back-scatters in the diffraction plane, allowing the following statement:

$$\sin(\theta_i) - \sin(-\theta_i - \epsilon) = \frac{m\lambda}{d \cos \psi} \quad (2)$$

Here, we define the projected, diffracted ray angle  $\theta_d = (-\theta_i - \epsilon)$ , where  $\epsilon$  encapsulates the projected angle of some particular diffracted ray relative to its central counterpart.

In order to continue the derivation, we will—from here on out—work under two key assumptions: (1) everything is to first order, ie.  $m = 1$ ; (2) if the final focusing mirror brings each EM ray onto the CCD plane at some

---

\* sdenglis@ucsc.edu

angle  $\epsilon$  at a horizontal position  $Z_{CCD}$  relative to pixel 381 (center), we can say that  $Z_{CCD} = \Delta(p - 381)$ , where  $\Delta = 9.00 \mu\text{m}$  is the pixel width. Thanks to the small angle approximation,  $\epsilon = Z_{CCD}/f$ , where  $f$  denotes the focal length of our mirror. Ultimately, the relationship between wavelength and CCD coordinate becomes

$$\sin(\theta_i) + \sin\left(\theta_i + \frac{\Delta(p - 381)}{f}\right) = \frac{m\lambda}{d \cos \psi} \quad (3)$$

This equation will yield values for  $\lambda$  given that we know  $\theta$ ,  $\Delta$ ,  $f$ ,  $d$ ,  $\psi$ , and the pixel number  $p$ . Lucky for us, the pixel width  $\Delta$ , grating constant  $d$ , out-of-plane angle  $\psi$  are all known to high accuracy (previously quoted).

$\theta_i$  can be empirically determined through a calibration process using two known wavelengths and solving as such:

$$\frac{\lambda_2 - \lambda_1}{p_2 - p_1} = \frac{d\Delta}{f} \cos \theta_i \cos \psi \quad (4)$$

Linear interpolation can then be used to show

$$\lambda(p) = \frac{(p - p_1)\lambda_2 - (p - p_2)\lambda_1}{p_2 - p_1} \quad (5)$$

By a simple re-arrangement of Eq.'s (3) & (5), we have two numerical implementations to precisely determine each  $\theta_i$  for a given micrometer setting as well as the focal length  $f$

$$\begin{aligned} \sin \theta_i &= \frac{\lambda(381)}{2d \cos \psi}, \\ f &= \frac{p_2 - p_1}{\lambda_2 - \lambda_1} d\Delta \cos \theta_i \cos \psi. \end{aligned} \quad (6)$$

### B. Micrometer Settings

In the previous subsection we discussed derivations for obtaining wavelengths and dealing with the calibration spectrum: if we now consider an adjustment to the micrometer, we will need to rethink how we obtain  $\theta_i$ . Namely, one can re-calibrate by solving Eq. (3) for its new value, using another calibration line ( $\lambda_1$ ,  $p_1$ ). Let  $p'_1 = (\Delta/f)(p_1 - 381)$  such that

$$\sin \theta_i + \frac{p'_1}{2} = \frac{\lambda}{2d \cos \psi \cos p'_1} \quad (7)$$

holds true. All captured spectra are taken at high resolution ( $\frac{1}{d} = 600$  lines per mm), where  $f$  is around 138 mm [4]. As soon as one gets a focal length  $f$ , they can then inspect data taken at various micrometer settings (different initial angle  $\theta$ ) by simply calibrating more wavelengths.

### C. Fraunhofer Lines

In order to properly identify absorption lines unique to our Sun, we must first understand what creates them in the first place. A spectral line, at its core, is a deviation in intensity from an otherwise uniform and continuous spectrum (resulting from emission or absorption of light in some frequency range). Spectral lines can often be used to identify specific atoms or molecules, due to each being associated with a unique “fingerprint” caused by quantum effects [5].

When a photon has just the right amount of energy (and thus, EM frequency), a system (some element) may spontaneously jump energy levels, later re-emitting the absorbed photon in a random direction and attenuating the EM energy seen from elsewhere: hence, absorption. For a star such as our Sun, it is filled with a combination of stellar materials which each interact with emitted energy (photons) in unique ways, thereby emitting and absorbing unique frequencies of light.

Fraunhofer lines [3] designate a unique value to strong spectral lines in the visible part of the spectrum (e.g. **H** at 3968.47 Angstrom, a singly-ionized calcium molecular marker), though some blend multiple lines from several different chemical species.

Fraunhofer lines result from gas in the photosphere of a star, the out-most region of where gas has relatively low temperatures compared to its inner radius counterparts [3]. We will use this conventional set of spectral absorption lines to aid us in identification of SGS's caught solar spectral features for our host, G-type main-sequence star.

### D. Error & Statistical Methods

During the laboratory experiment, we noticed a shift in the central wavelength compared to the expected for any given micrometer setting. After having looked at all spectra, we find that the central wavelengths were roughly 300 Angstroms less than expected (although this varies by some 50 Angstrom).

This is important to note, but not detrimental to the calculations and identification of solar spectral features we wish to conduct. Systemic error of this nature pushes us to be more cognisant and to record data for the 7.2 mm micrometer setting.

On the other hand, there is a significant and unavoidable presence of human bias associated with the manual deduction of spectral feature locations (i.e. we had no automated process to determine the precise location of each peak or trough).

Because of this, we will inherently sway our calculated values to one direction or the other since each tabulated wavelength is very sensitive to the CCD pixel coordinates. A small shift in pixel count from one bin to the next will cause roughly a doubling in the relative error. It would be unfair to say that our results are not affected by this: a better approach may be to inflate our standard

deviation by some amount such that our results are not unintentionally misleading.

We hope future works implement an automated process or algorithm to systematically treat each peak and trough such that its own bias becomes consistent and can be deftly accounted for.

Beyond these experimental and systematic errors, we have simple entries for relative wavelength error and percent error, quoted to the literature's significance of six digits as seen in Fig. 1.

## II. APPARATUS AND PROCEDURE

Santa Barbara Instrument Group (SBIG) kindly allowed our research team to utilize their Self Guided Spectrograph (SGS) and spectra analysis software to capture stellar spectra with high resolution, sensitivity as well as flexibility [4].

In total, we took 14 unique measurements of spectra with SGS. These files can be divided into further camps: solar spectra for analysis and Mercury-Argon arc lamp spectra for calibration. With each type inheriting its respective half of the data sets, we note that our experiment ran the micrometer from 4.0 mm to 7.2 mm (to ensure encapsulation of all markers wanted due to an apparent offset in our micrometer's value, Sec. ID).

For each setting, using an ancient Windows laptop running camera control software, our CCD would pickup spectral features through the spectrograph housing.

The Python analysis goes as follows:

1. Crop SGS's 2D data into a 1D intensity vs. pixel (for both solar spectra and calibration files)
2. Determine the effective focal length of the collimating mirror. To do this, use the mercury-argon calibration spectrum.
  - (a) If two or more distinct peaks are visible:
    - i. Using your estimate for the central wavelength, make educated predictions as to the wavelength associated with the two peak pixel intensity values.
    - ii. Using these two values, ensure the focal length  $f$  is correct (roughly 138 mm).
    - iii. Once confirmed, calculate the central angle  $\theta$ .
  - (b) If a single peak (or none) are present:
    - i. Assume  $f$  of previous calculations.
    - ii. We know the dispersion is linear: it can be shown that the relationship between  $\theta_i$  and micrometer setting is linear. Take the values of  $\theta$  we do know to interpolate for the missing value.
    - iii. As a last resort: identify prominent features from the solar spectra to calibrate.

(c) NOTE: SGS's raw spectra run from large (red) on the left to smaller (blue) wavelengths on the right. Please be aware.

3. Using the pixel to wavelength calibration from Step 2, one can find the wavelengths associated with any absorption line visible in the solar spectra.

We are to identify a minimum of ten lines in the Sun's photosphere to inform us about the composition and subsequent complex interactions occurring inside of our solar system's stellar host. As Sec. IC discussed, Fraunhofer lines [3] are an excellent foundational list of features in the Sun's spectrum.

## III. RESULTS AND DISCUSSION

### A. Tabulated Values

After closely following the procedure outlined in Sec. II and much tabulation, we managed to identify a set of fifteen absorption lines in our Sun's photosphere: we find that our SBIG-borrowed SGS could accurately re-discover Fraunhofer lines [3] in the order of **K** [Ca<sup>+</sup>], **H** [Ca<sup>+</sup>], **h** [H $\delta$ ], **G'** [H $\gamma$ ], **e** [Fe], **F** [H $\beta$ ], **b<sub>4</sub>** [Mg], **b<sub>2</sub>** [Mg], **b<sub>1</sub>** [Mg], **E<sub>2</sub>** [Fe], **D<sub>2</sub>** [Na], **D<sub>1</sub>** [Na], **a** [O<sub>2</sub>], **C** [H $\alpha$ ], and **B** [O<sub>2</sub>]. Respectively, each spectral absorption line falls at known literature (expected) values in units of Angstrom: 3933.66, 3968.47, 4101.75, 4340.47, 4383.55, 3861.34, 5167.33, 5172.70, 5183.62, 5270.39, 5889.95, 5895.92, 6276.61, 6562.81, 6867.19 (see Fig. 1).

Values for our measured wavelengths matched incredibly well, with no signature rising above 0.025% error. Focal lengths stayed tried and true to our expected value of 138 mm; the central angle  $\theta$  followed a linear trend with micrometer setting, as predicted by theory.

Fig. 3 visually illustrates the calibration process with our mercury-argon lamp; for every subplot, the wavelength(s) of each spectra is given for intensity vs. CCD pixel coordinate. A maximum of two peaks were used for each micrometer setting (4.0, 4.4, ..., 7.2 mm). Our 6.2 mm micrometer setting yielded an unruly amount of background noise. Despite this, along with thermal noise, photon bleeding, etc., Sec. II's methods reliably produce a steady calibration and subsequent identification of solar spectral features.

Likewise, Fig. 2 depicts each established solar absorption line micrometer setting to setting (4.0, 4.4, ..., 7.2 mm). For each subplot of photon intensity vs. pixel coordinate, we pinpoint at least a single spectral feature for our Sun; one could verify the legitimacy of our claims by inspection, perhaps comparing to previous works or one's own to reaffirm our results. For someone well-acquainted with spectroscopy, picking out the sodium doublet [1] (**D<sub>1</sub>** [Na], **D<sub>2</sub>** [Na]) or simply emission lines of the Balmer series (**C** [H $\alpha$ ], **F** [H $\beta$ ], **G'** [H $\gamma$ ]) is a quick and easy verification.

Discrepancy (or lack thereof) between calculated and expected could very well be caused in part by the experimental biases discussed in Sec. ID.

### B. Solar Composition Implications

Ideally, we could obtain some normalized intensity of every solar feature identified, thereby yielding a relative abundance of each gaseous substance within our Sun’s photosphere. However, this calculation is beyond the scope of our experiment: we look to future papers for results supporting a breakdown of stellar compositions.

In fact, very promising work has already been conducted in Schmidt, et. al. [6], where authors exploit machine learning to automatically identify stellar chemical species given exorbitantly large data sets. Although their analysis tool leaves precise quantification is out of scope, it can be used to quickly and efficiently summarize a data-set, giving end-members and their abundances to help discover new minor species.

As of now, we can only state that our Sun contains some compositional distribution of elements calcium, hydrogen, iron, magnesium, sodium, and oxygen (with

the highest abundance expected to be hydrogen due to hydrogen-burning as a main-sequence star [2]).

## IV. CONCLUSIONS

We have successfully identified fifteen Fraunhofer absorption lines in our Sun’s photosphere using SBIG’s SGS machinery and analysis software. While we cannot state with certainty the relative abundances of each chemical species, we can definitively conclude the *presence* of singly-ionized calcium (*see Fig. 1*), hydrogen, magnesium, iron, sodium, and oxygen. One might expect to see an abundance of hydrogen (and helium, both contributing roughly 95%+ put together) given that our host star is on the main sequence (MS); furthermore, heavier elements are known to account for only a small portion ( $\ll 5\%$ ) of MS photospheric composition [2].

Relative errors on any given signature’s wavelength do not exceed 0.025%, yet cannot be entirely certified given the nature of our experimental tabulation. Human bias played a crucial role in our identification of solar spectral features. Future work needs to account for these biases with the aid of some automated algorithm implementation.

---

## ACKNOWLEDGMENTS

SE is a part of the ASTR 135, Advanced Laboratory course. None of this information is presented for journal publication, only for writing improvement.

## BIBLIOGRAPHY

- [1] Corn, Robert. Analytical Spectroscopy: “The Sodium D-lines”, RWFSodium.pdf (2020).
- [2] “The Sun’s Vital Statistics”. Stanford Solar Center. Retrieved 29 July 2008. Citing Eddy, J. (1979). A New Sun: The Solar Results From Skylab. NASA. p. 37. NASA SP-402.
- [3] Fraunhofer, J. (1817). Denkschriften der Königlichen Akademie der Wissenschaften zu München, V, 193-226.
- [4] Holmes, Alan. (2001). Operating Instructions for the Santa Barbara Instrument Group: Self Guided Spectrograph & Spectra Analysis Software.
- [5] Jenkins, Francis A.; White, Harvey E. (1981). Fundamentals of Optics (4th ed.). McGraw-Hill. p. 18. ISBN 978-0-07-256191-3.
- [6] Schmidt et al., “Machine learning for automatic identification of new minor species”, Journal of Quantitative Spectroscopy and Radiative Transfer, arXiv:2012.08175 (January 2021).

## APPENDIX

	Measured Wavelength (Å)	Literature Wavelength (Å)	Error (Å)	Error (%)	Focal Length (mm)	$\theta$ (rad)
<b>K [Ca+]</b>	3934.13	3933.66	0.466	0.012	138.30	0.111
<b>H [Ca+]</b>	3969.41	3968.47	0.935	0.024	138.30	0.111
<b>h [Hδ]</b>	4102.23	4101.75	0.476	0.012	138.55	0.124
<b>G' [Hγ]</b>	4340.63	4340.47	0.156	0.004	138.55	0.124
<b>e [Fe]</b>	4384.26	4383.55	0.706	0.016	138.36	0.137
<b>F [Hβ]</b>	4862.06	4861.34	0.718	0.015	138.36	0.137
<b>b4 [Mg]</b>	5167.10	5167.33	0.231	0.004	138.46	0.150
<b>b2 [Mg]</b>	5172.41	5172.70	0.289	0.006	138.46	0.150
<b>b1 [Mg]</b>	5183.03	5183.62	0.587	0.011	138.46	0.150
<b>E2 [Fe]</b>	5270.15	5270.39	0.24	0.005	138.46	0.162
<b>D2 [Na]</b>	5890.47	5889.95	0.523	0.009	138.33	0.174
<b>D1 [Na]</b>	5896.83	5895.92	0.911	0.015	138.33	0.174
<b>a [O2]</b>	6278.15	6276.61	1.54	0.025	138.44	0.186
<b>C [Hα]</b>	6563.51	6562.81	0.7	0.011	138.32	0.198
<b>B [O2]</b>	6868.44	6867.19	1.25	0.018	138.23	0.210

Figure 1. Tabulated values associated with the Sun's solar spectra taken with SBIG's SGS [4]. Each Fraunhofer absorption line [3] recorded contains measured wavelength (with CCD calibration from mercury-argon lines), an expected literature wavelength given by theory, relative error and percent error, focal length used for a particular sub-spectra, and central angle  $\theta$  associated with a given micrometer setting. Green colors indicate size of error: darker cells imply a heavier error or percentage. Blue shaded cells for  $\theta$  group together micrometer settings (4.0, 4.4, ..., 7.2 mm). For example: **K** and **H** were recorded in tandem for the 4.0 mm micrometer configuration; hence, they both use the same focal length  $f = 138.30$  as well as central angle  $\theta = 0.111$ .

## Sun Spectra

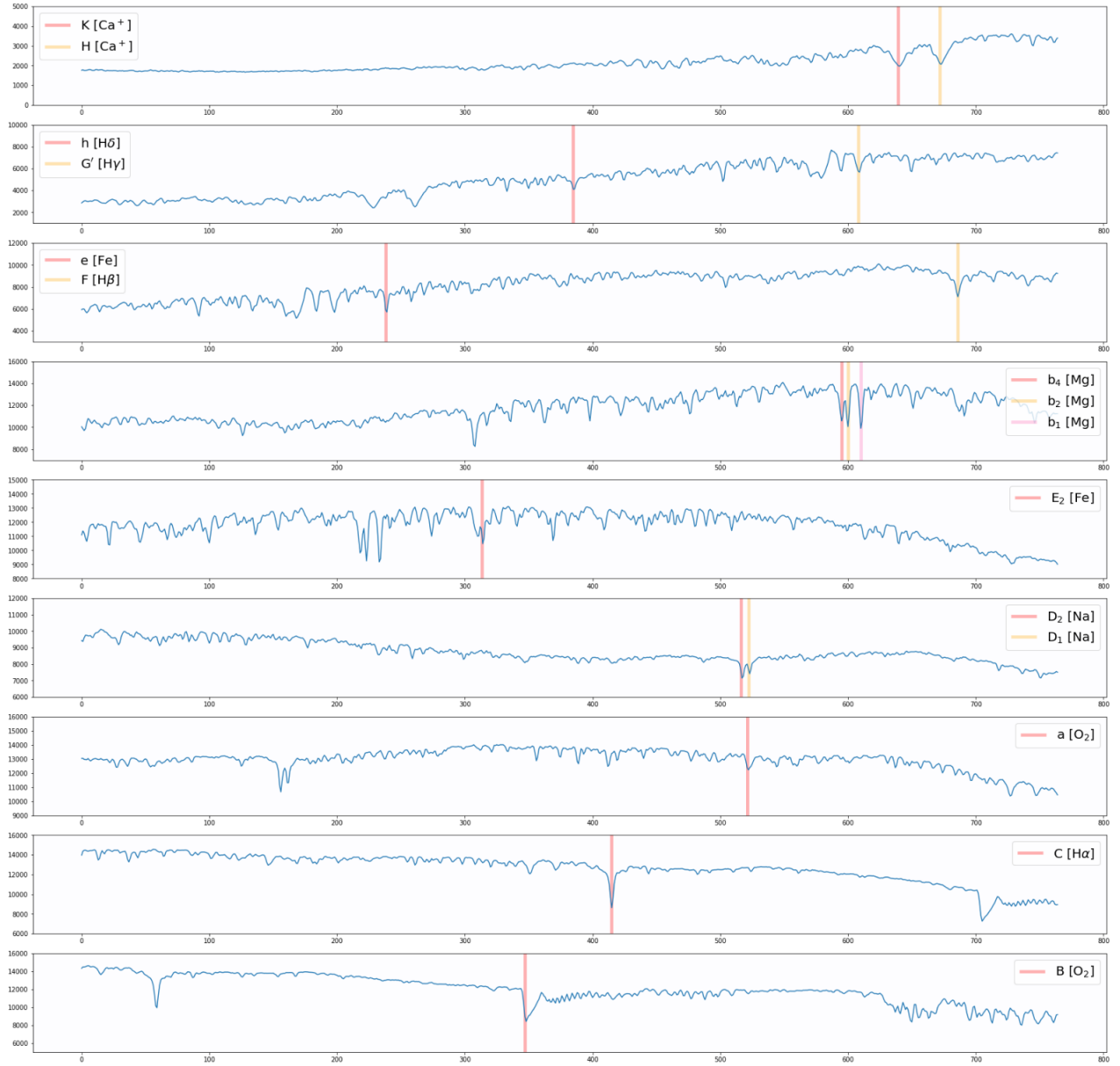


Figure 2. Finalized solar spectra from our Sun using the SGS [4]. Each subplot illustrates the photon signal intensity vs. CCD pixel coordinate over a range of wavelengths for a given micrometer setting (4.0, 4.4, ..., 7.2 mm). Vertical colored bars indicate which Fraunhofer lines [3] correspond to what absorption features. *For example*: a set of modest sodium D-lines, which visually display a bright yellow emission for 6.0 mm (sixth plot from top). These markers can even be used to [1] measure Doppler shifts and the size of the universe! Detailed measured and expected wavelengths are given in Fig. 1.

## Mercury Spectra

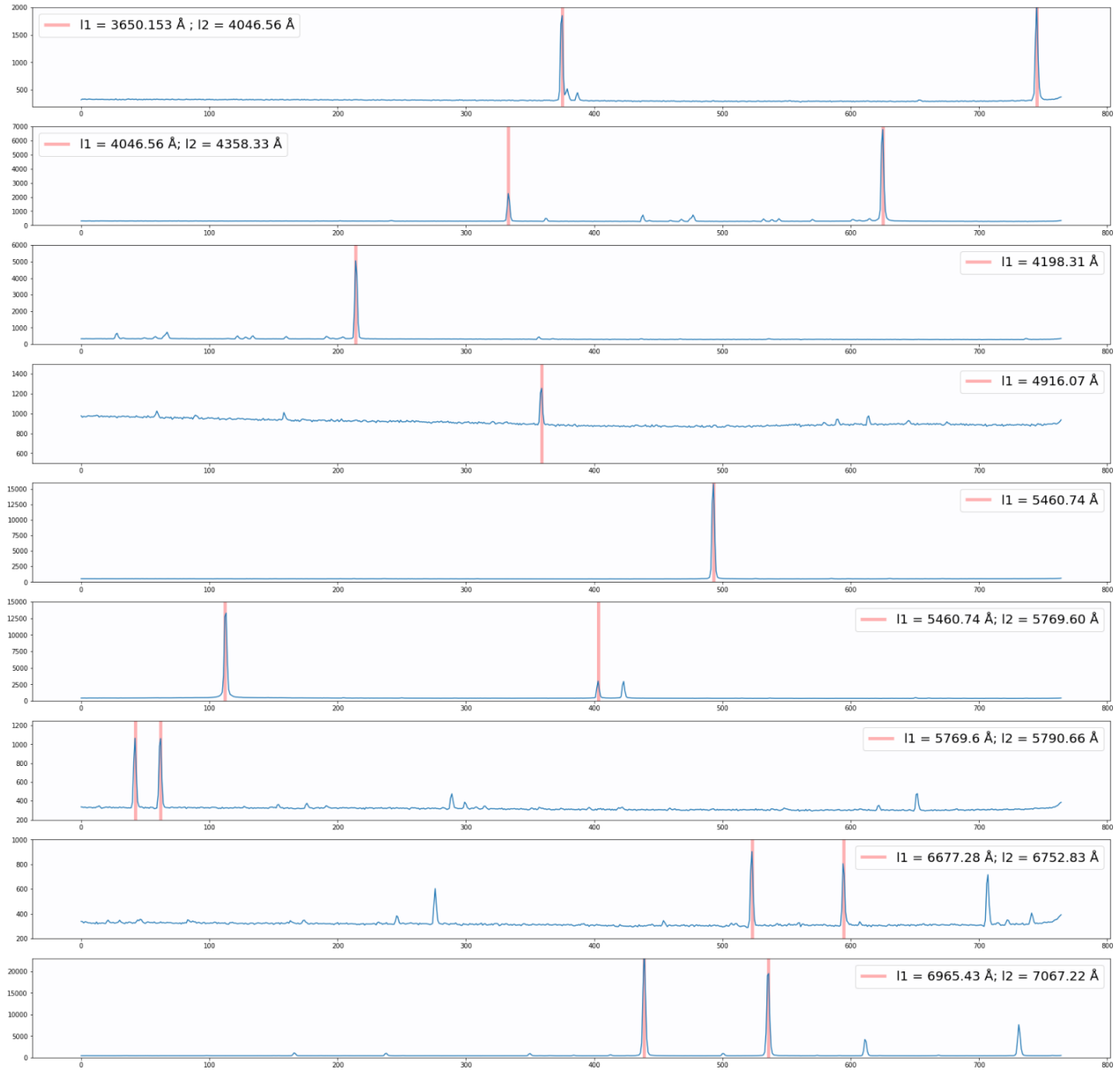


Figure 3. Finalized mercury-argon spectra from our calibration lamp using the SGS. Each subplot illustrates the photon signal intensity vs. CCD pixel coordinate over a range of wavelengths for a given micrometer setting (4.0, 4.4, ..., 7.2 mm). Vertical colored bars indicate which measured wavelengths were used to calibrate focal length  $f$  and central angle  $\theta$ . Expected wavelengths are given in Fig. 4.

ELEMENT	WAVELENGTH (Å)
Hg	3650.15
Hg	4046.56
Hg	4077.83*
Ar	4158.59*
Ar	4198.31*
Hg	4358.33
Hg	4916.07*
Hg	5460.74
Hg	5769.60
Hg	5790.66
Ar	5888.58*
Ar	5912.08*
Ar	6032.13*
Ar	6043.22*
Ar	6384.71*
Ar	6416.31*
Ar	6604.28*
Ar	6677.28*
Hg	6716.43
Ar	6752.83*
Ar	6871.29*
Hg	6907.32
Ar	6965.43
Ar	7030.25
Ar	7067.22
Ar	7147.04

Figure 4. Mercury-Argon lamp lines observed (SPECTRA database). Mercury lamp used has trace amounts of argon.